

Biopathways Representation and Simulation on Hybrid Functional Petri Net

Hiroshi Matsuno¹, Hitoshi Aoshima¹, Atsushi Doi¹, Yukiko Tanaka¹, Mika Matsui²,
Satoru Miyano³

¹Faculty of Science, Yamaguchi University, ²Oshima National College of Maritime Technology, ³Human Genome Center, Institute of Medical Science, University of Tokyo

Received: date / Revised version: date

Abstract. The following two matters should be resolved for biosimulation tools in order to be accepted by users in biology/medicine; (1) Remove issues which are irrelevant to biological importance, and (2) Allow users to represent biopathways intuitively and understand/manage easily the details of representation and simulation mechanism. From these criteria, we firstly define a novel notion of Petri net called *hybrid functional Petri net* (HFPN). Then, we introduce a software tool, *Genomic Object Net*, for representing and simulating biopathways, which we have developed by employing the architecture of HFPN.

In order to show the effectiveness of *Genomic Object Net* for representing and simulating biopathways, we show some typical biopathway modelings related to gene regulation (switching mechanism of λ phage, circadian rhythm of *Drosophila*, lacoperon regulatory mechanism of *E. coli*), metabolic pathway (glycolytic pathway), and signal transduction (Fas ligand induced apoptosis)), which cover the basic aspects in biopathways.

The software is available to academic users from <http://www.GenomicObject.Net>.

formalisms, applications, data sources, visualizations, simulations, and nexus (information coordination) to foster and support the development of technologies and open standards for representing, handling, accessing, analyzing, and adding value to pathways and protein interaction information. Among many issues in this approach, a vital necessity is to develop information technology with which we can easily model the structurally complex dynamic causal interactions and processes of various biological objects such as genomic DNA, mRNA, proteins, functional proteins, molecular transactions and processes such as metabolic pathways, signal transduction cascades, genetic networks, etc.

Considerable attentions have been paid to the biopathway representation and simulation in the literature. The most traditional approach is to employ ordinary differential equations (ODEs) such as Michaelis-Menten equations and to represent biochemical reactions as a systems of ODEs. Especially, the metabolic control analysis has been well established for many years on the ODE modeling [12, 13] as well as the graph theoretical modeling [19] and discrete-event technique [29]. This approach provides mathematically well-founded and fine interpretations of biopathways as well as stochastic kinetic approach [2, 26]. Gepasi [28] is a software package based on this approach for modeling biochemical systems and it aims at assisting users in translating reaction processes to matrices and ODEs. E-Cell [37, 39] develops a system for representation and simulation with GUI. A system of reactions is represented with a spread sheet compiling substances and reactions with ODEs. For reactions which cannot be represented with ODEs, it employs *ad hoc* user-defined C++ programs. With E-Cell, Tomita et al. [40] tried to model several biopathways including biochemical reactions in human erythrocyte, signal transduction for bacterial chemotaxis, energy metabolism in mitochondria and lytic-lysogenic switch network of λ phage. Unfortunately, it is rather complicated to use E-

1 Introduction

Along with the completion of many genome sequencing projects, a new interest of research is emerging for elucidating how the living systems function in terms of all levels of biological information, and then to develop information technology for applying such systemic information to medicine and biology, as is suggested in the notion of Systems Biology [34] and KEGG project [20].

This approach requires to handle the information about gene functions in the whole context of cellular mechanisms. For this purpose, the Biopathway Consortium [44] has organized working groups for investigating

Cell for modeling even simple biopathways. The switching mechanism of the λ phage is also simulated with LISP language description [14] where knowledge about the biopathway is elegantly represented with LISP and is simultaneously simulated with LISP system. BioSpice [45] is a similar system whose idea is to regard biopathways as electrical circuits (SPICE is a very commonly used software tool for electrical circuit design). BioDrive [23] is a system taking account of aspects in multicellular organisms. Kyoda et al. [23] have modeled the *Drosophila* Smad signal transduction pathway and succeeded in reconstructing the spacio-temporal patterning of gene products, proteins and their complexes. These systems may be useful if focused on kinetics. But some *ad hoc* features are required to enhance the systems if the scope is not on kinetics. It is also our experience that the utility and accessibility to users in biology/medicine may not be enough satisfactory.

Reflecting such defects in the above systems, Scharff and Loew [33] and Stelling et al. [35] have intended to develop a general computational framework for experimentalists to create models and to generate predictions from models via simulations. In Virtual Cell [33], a model is defined as a collection of species (e.g. calcium, ATP), reactions (e.g. enzyme kinetics, receptor binding) and features (e.g. ER, cytosol), and ODEs for kinetic reactions and PDEs for diffusive objects are employed. In Virtual Biological Laboratory, Stelling et al. [35] took an object-oriented approach and have been developing process modeling tool PROMOT by defining a graphical language which gives a modeling concept that allows for easy model development and interpretation. A simulation environment DIVA [25] is used for dynamic simulation, parameter estimation and model analysis.

As is stressed in [35] and [36], in order for software tools to be accepted by users in biology/medicine for biopathway modeling, we consider the following two matters should be resolved, at least: (1) Remove issues which are irrelevant to biological importance; Otherwise, users might be trained to understand some special notions in mathematics, physics and computer science which are irrelevant to biology/medicine. (2) Allow users to represent biopathways intuitively and understand/manage easily the details of representation and simulation mechanism; Otherwise, users could not have a confidence that the understanding and knowledge in their minds coincides with the object represented with the software tools.

From these criteria, in this paper we firstly define a novel notion of Petri net called *hybrid functional Petri net* (HFPN) by extending the notions of hybrid Petri net [1], functional Petri net [42] and hybrid object net [3] so that the notion will be suited for modeling biopathways. This extension was made from a viewpoint of biopathway modeling by identifying, inheriting and resolving the merits and demerits of Petri nets so far defined as follows:

1. The original Petri net deals with discrete amounts and is suitable for stepwise switching mechanisms and cases that the amounts can be counted as integers. HFPN inherits all the aspects of the original Petri net.
2. Hybrid Petri net allows continuous feature of amounts in addition to the original ability of Petri net. Thus ODEs can be realized very intuitively and easily. But dynamic changes of the network structure is not possible. Lack of this ability becomes a vital drawback in biopathway modeling and HFPN is defined to have this ability.
3. Functional Petri net allows dynamic changes of the network structure to some extent, but only deals with discrete amounts. HFPN is defined to include the extension of this ability.
4. Hybrid object net is defined by enhancing hybrid Petri net with hierarchization in the network structure. The hierarchization is useful in describing complex network structures and this is inherited to HFPN.
5. The research on Petri net has a history of more than 30 years and it is mathematically well-founded and practically well-established. The simulation system of HFPN can fully benefit from this Petri net research.

Then, we introduce a software tool, *Genomic Object Net*, for representing and simulating biopathways, which we have developed by employing the architecture of HFPN. We shall discuss the ability of HFPN in Section 2. *Genomic Object Net* has an editor and a simulator of HFPN with GUI which shall resolve the matters (1) and (2). In order to show the effectiveness of *Genomic Object Net* for representing and simulating biopathways, we show some typical biopathway modelings related to gene regulation (switching mechanism of λ phage, circadian rhythm of *Drosophila*, lacoperon regulatory mechanism of *E. coli*), metabolic pathway (glycolytic pathway), and signal transduction (Fas ligand induced apoptosis), which cover the basic aspects in biopathways. It is not the purpose of this paper to tune precisely the parameters appearing in the biopathways, but to show that *Genomic Object Net* would be a useful tool satisfying mostly the above criteria in practice.

Usually, a biopathway information is conceptually described as a figure like Figure 9 (a) together with the explanation about the relations between biological objects of concern and the measured/observed data proving their qualitative/quantitative relations. For such biopathway information, we first show a design principle for modeling biopathways with *Genomic Object Net* with its visualization facility of HFPN and simulation environment. The above biopathways used for qualifying *Genomic Object Net* are described quite easily by following this design principle. The current version of *Genomic Object Net* does not equip the automatic/semi-automatic mechanism of tuning or discovering parameters in the biopathways which shall make optimal fitting of the parameters to the measurements/observations. By using

biological/biochemical knowledge, however, we could attain the level that simulation results are good enough to explain the known biopathway information.

This paper is organized as follows: Section 2 defines HFPN and some remarks in representing biopathways with HFPNs and gives a snapshot of the software *Genomic Object Net* (ver. 0.919) ¹ In Section 3, we shall show representations and simulations of three biopathways: *lac* operon gene regulatory mechanism with the glycolytic metabolic pathway, circadian rhythm gene regulatory network of *Drosophila*, and Fas ligand induced apoptosis signaling network. Section 4 discusses the current limitations of *Genomic Object Net* and issues for further extensions.

2 Modeling of Biological Systems with Hybrid Functional Petri Net

2.1 Hybrid Functional Petri Net

By reviewing the notion of Petri net, we firstly show how the general notion of Petri net has been applied to represent and simulate biopathways. Then we introduce the *hybrid functional Petri net* (HFPN) model as the most general Petri net model, which is realized in *Genomic Object Net* for modeling and simulating various biopathways. With this tool, an interesting software tool such as E-Cell [37] can be realized as a subset of Genomic Object Net. The stochastic feature is also an important element in biological systems. However, the current Genomic Object Net does not implemented the stochastic features like the stochastic Petri net model [8,9] and it remains as the next feasible task.

Definition of HFPN

In general, a *Petri net* is a network consisting of the following four kinds of elements (see Figure 1): (1) place, (2) transition, (3) arc, (4) token. A *place* can hold *tokens* as its content. A *transition* has arcs coming from places and arcs going out from the transition to some places. A transition with these arcs defines a *firing rule* in terms of the contents of the places where the arcs are attached.

In the *discrete Petri net model*, a nonnegative integer (the number of tokens) is used for representing the content of the place. Instead of giving a formal definition of a transition in the discrete Petri net model, we show a typical example in Figure 1 together with its explanation.

Reddy et al. [32] employed the discrete Petri net for modeling metabolic pathways where places represent biological compounds (metabolites), transitions represent chemical reactions between metabolites which are usually catalyzed by a certain enzyme, and tokens indicate

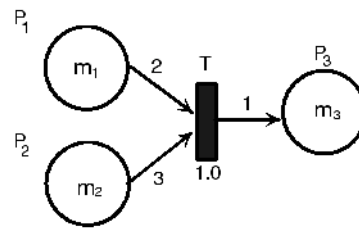


Fig. 1. We call places P_1 and P_2 *input places* and P_3 an *output place* of transition T . The contents of places P_1 , P_2 and P_3 are m_1 , m_2 and m_3 , respectively. The constant weights 1 and 2 on the arcs from P_1 and P_2 and the number 1.0 attached to transition T mean that T can fire if $m_1 \geq 2$ and $m_2 \geq 3$ and it will fire after delay $d = 1.0$ time unit. By firing, 2 tokens are removed from P_1 , 3 tokens are removed from P_2 and 1 token is added to P_3 . The weight and delay must be constant in the discrete Petri net model. If two transitions share the same place as their input place, there may occur a conflict in firing which depends on the amount of the content of the input place. When a place is shared by two transitions as their output place, the place will get contributions from both transitions.

the presence of compounds. The approach by Reddy et al. [32] is based on the condition event mechanisms and the discussions were made only on *qualitative* aspects. That is, a place having token(s) only represents the presence of the corresponding compound to the place, no matter how many tokens are contained in the place. Hofestadt expanded Reddy’s idea to model metabolic processes [15].

Hofestadt and Thelen [16] tried to make *quantitative* simulations by using the self-modifying Petri net model [42] where the number of token(s) in a place is used to represent the level of concentrations of the corresponding compound. The main feature of the self-modifying Petri net is that the content of a place can be used as a parameter for the formula describing the weight on the arc from the place that represents the threshold and consumption of tokens for firing. With this modification, biochemical processes are modeled with actual concentrations. Moreover, in order to represent more complex relations and conditions, they used the functional Petri net where the calculation of the dynamic biocatalytic processes can be realized by using functions for specifying the arc weight. By using Design/CPN, which is a well known tool based on high level Petri net technique, modeling and simulating metabolic pathways are carried out [6,11].

Ordinary differential equations (ODEs) are widely accepted to express biological phenomena such as biochemical reactions. But in this approach, it is rather difficult to observe the whole system intuitively like a picture if the system constitutes a large network of cascades. Although the discrete Petri net model allows very intuitive graphical representation, the mechanism of ODEs

¹ This software can be downloaded from the URL <http://www.GenomicObject.Net/>.

cannot be directly realized because the discrete Petri net model deals with only integers as the contents of places. For sophisticated dynamic systems in which control mechanisms of genes and chemical reactions with enzymes are concurrently performed, it is more reasonable to use real numbers for representing the amounts of some objects, e.g. the concentrations of a protein, mRNA, complex of proteins, metabolites, etc.

The hybrid Petri net model (HPN) [1] has been introduced as an extension of the discrete Petri net model so that it can handle real numbers in the continuous way and it allows us to express explicitly the relationship between continuous values and discrete values while keeping the good characteristics of discrete Petri net soundly. Drath [3,4] has also enhanced this notion to define the hybrid dynamic net model (HDN) for modeling more complex systems.

In HPN/HDN model, two kinds of places and transitions are used, *discrete/continuous places* and *discrete/continuous transitions*. A discrete place and a discrete transition are the same notions as used in the discrete Petri net model. A continuous place holds a nonnegative real number as its content. A continuous transition fires continuously in the HPN/HDN model and its firing speed is given as a function of values in the places in the model. For graphical notations, discrete transition, discrete place, continuous transition and continuous place are drawn as shown in Figure 4. An example of continuous transition is shown in Figure 2. Another example of a continuous transition is shown in Figure 3 that represents the Michaelis-Menten's equation.

From the definition of HPN/HDN, the firing speed of a continuous transition must be the same as the consuming speed through each arc from its source place and the contents of all source places are consumed with the same speed. This speed is also the same as the production speed through each arc from the transition. This is the unfavorable feature of HPN/HDN for biopathway simulation. For example, consider a reaction in which a dimer is cleaved to two monomers (Figure 6 (a)). This reaction in the HDN model could be represented as shown in Figure 6 (b) by using a test arc and a transition for amplification (note that the amounts consumed and produced in places by continuous transition firing is the same by definition while the amount of monomers is twice as large as that of dimers). But it is neither intuitive nor natural at all. It may be obvious that this feature of HPN/HDN is a severe drawback in modeling biopathways.

On the other hand, some favorable features have been also introduced in Petri net theory. In addition to normal arc explained so far, *inhibitory arc* and *test arc* have been defined for convenience (Figure 4). An inhibitory arc with weight r enables the transition to fire only if the content of the place at the source of the arc is less than or equal to r . For example, an inhibitory arc can be used to represent the function of “repress” in gene

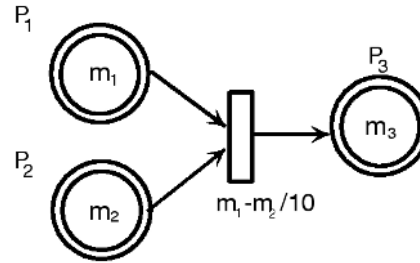


Fig. 2. P_1 , P_2 and P_3 are continuous places whose contents are represented by m_1 , m_2 and m_3 , respectively. We draw a continuous place as a double circle while a discrete place is drawn as a single circle. A function $m_1 - m_2/10$ is assigned to continuous transition T as its firing speed. T can fire if $m_1 > 0$ and $m_2 > 0$ (in the original definition of the hybrid dynamic net, this condition is not necessary). When T is firing, the contents of P_i will be consumed through the arc from P_i to T with speed $m_1 - m_2/10$ for each $i = 1, 2$ and the content of P_3 will be increased through the arc from T to P_3 with the same speed.

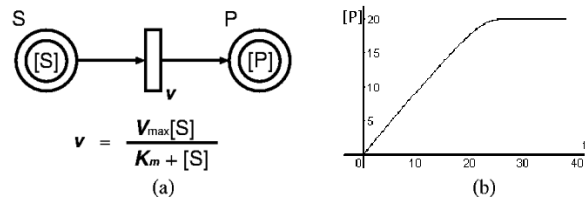


Fig. 3. (a) Let $[S]$ and $[P]$ be the contents of continuous places S and P , respectively. v is a continuous transition whose firing speed is given by the function (enzyme reaction speed) $\frac{V_{\max} \cdot [S]}{K_m + [S]}$, where V_{\max} is a constant number representing the maximum reaction rate and K_m is the Michaelis constant. It fires under the condition $[S] > 0$ and $[S]$ will be decreased and $[P]$ will be increased with the speed $\frac{V_{\max} \cdot [S]}{K_m + [S]}$, i.e. $-\frac{d[S]}{dt} = \frac{d[P]}{dt} = \frac{V_{\max} \cdot [S]}{K_m + [S]}$. (b) The behavior of continuous place P for $V_{\max} = 1$ and $K_m = 1$.

regulation (see Figure 9). A test arc does not consume any content of the place at the source of the arc by firing. For example, test arcs can be used to represent the transcription process since nothing is consumed by this process except for degradation. An operon consisting of *gene1* and *gene2* in Figure 5 (a) can be represented as shown in Figure 5(b) with test arcs.

From these considerations, we define the following new notion by inheriting merits from HPN/HDN and by resolving the drawback of HPN/HDN.

Definition 1. A *hybrid functional Petri net* (HFPN) is defined by extending the notion of transition of HPN/HDN [1,3,4] in the following way: HFPN has five kinds of arcs; *discrete input arc*, *continuous input arc*, *test input arc*, *discrete output arc*, and *continuous output arc*. A discrete input arc (continuous input arc) is directed to a discrete transition (continuous transition) from a dis-

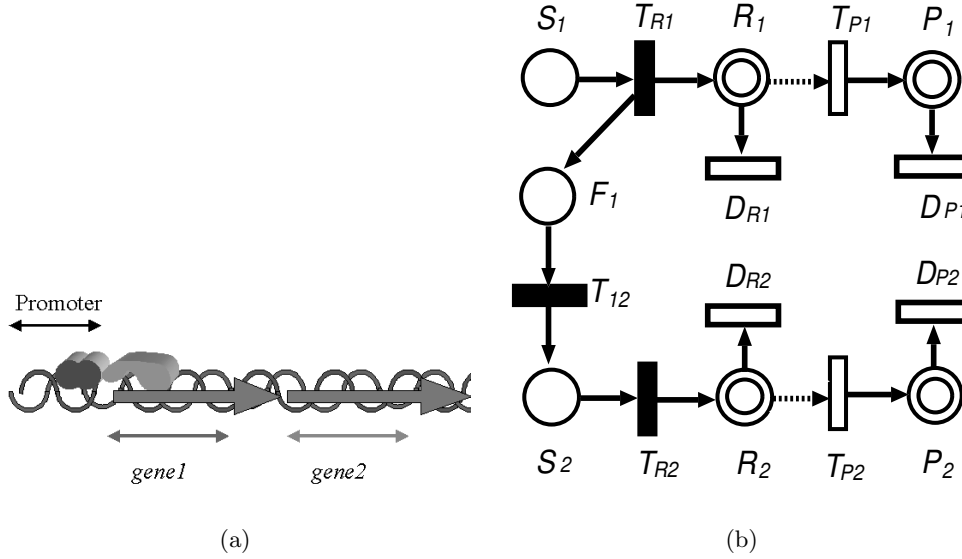


Fig. 5. (a) An operon consisting of two genes, *gene1* and *gene2*. (b) HPN model for two-gene operon model: At the beginning, discrete place S_1 has a token (this reflects the situation that RNA polymerase binds to the promoter of the operon), whereas any other place contains the value 0. Note that S_1 (S_2) works as a switch for transcription of *gene1* (*gene2*). The time for transcription of *gene1* (*gene2*) is assigned to the discrete transition T_{R1} (T_{R2}) as a delay time. The continuous place R_1 (R_2) contains a concentration of *gene1* (*gene2*) and the continuous place P_1 (P_2) contains a concentration of the protein of *gene1* (*gene2*). The test arc is used from R_1 (R_2) to continuous transition T_{P1} (T_{P2}) whose firing produces protein of *gene1* (*gene2*). Usage of these test arcs reflects that mRNA is not consumed in the translation process. At the continuous transition T_{P1} (T_{P2}), the speed representing rate of translation is given. The continuous transitions D_{R1} (D_{R2}) and D_{P1} (D_{P2}) have parameters representing rate of degradations of mRNA and protein of *gene1* (*gene2*), respectively. The discrete transition T_{12} has a parameter representing the time required for RNA polymerase to move from *gene1* to *gene2*.

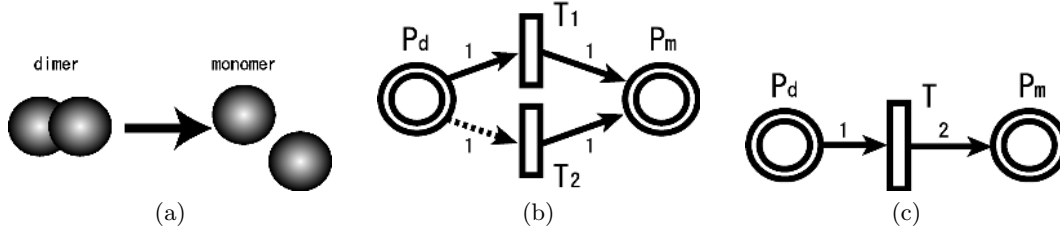


Fig. 6. Model for reaction decomposing dimers to monomers. (a) Reaction decomposing dimers to monomers. (b) Hybrid Petri net. (c) Hybrid functional Petri net.

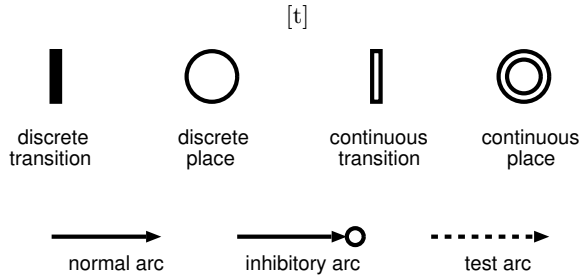


Fig. 4. Basic elements of hybrid Petri net.

crete/continuous² place (continuous place) from which it consumes the content of the source place by firing. A test input arc is directed from a place of any kind to a transition of any kind. It does not consume the content of

the source place. These three arcs are called *input arcs*. A discrete output arc is directed from a discrete transition to a place of any kind. A continuous output arc is directed from a continuous transition to a continuous place. These two arcs are called *output arcs*.

- (1) Continuous transition: A *continuous transition* T of HFPN consists of continuous/test input arcs a_1, \dots, a_p from places P_1, \dots, P_p to T and continuous output arcs b_1, \dots, b_q from T to continuous places Q_1, \dots, Q_q . Let $m_1(t), \dots, m_p(t)$ and $n_1(t), \dots, n_q(t)$ be the contents of P_1, \dots, P_p and Q_1, \dots, Q_q at time t , respectively. The continuous transition T specifies the following:

- (a) The *firing condition* given by a predicate $c(m_1(t), \dots, m_p(t))$. As long as this condition is true, T fires continuously.
- (b) For each input arc a_i , T specifies a function $f_i(m_1(t), \dots, m_p(t)) \geq 0$ which defines the speed

² A/B means A or B.

of consumption from P_i when it is firing. If a_i is a test input arc, then we assume $f_i \equiv 0$ and no amount is removed from P_i . Namely, $d[a_i](t)/dt = f_i(m_1(t), \dots, m_p(t))$, where $[a_i](t)$ denotes the amount removed from P_i at time t through the continuous input arc a_i during the period of firing.

- (c) For each output arc b_j , T specifies a function $g_j(m_1(t), \dots, m_p(t)) \geq 0$ which defines the speed of amount added to Q_j at time t through the continuous output arc b_j when it is firing. Namely, $d[b_j](t)/dt = g_j(m_1(t), \dots, m_p(t))$, where $[b_j](t)$ denotes the amount of the contents added to Q_j at time t through the continuous output arc b_j during the period of firing.
- (2) Discrete transition: A *discrete transition* T of HFPN consists of discrete/test input arcs a_1, \dots, a_p from places P_1, \dots, P_p to T and discrete output arcs b_1, \dots, b_q from T to places Q_1, \dots, Q_q . Let $m_1(t), \dots, m_p(t)$ and $n_1(t), \dots, n_q(t)$ be the contents of P_1, \dots, P_p and Q_1, \dots, Q_q at time t , respectively. The discrete transition T specifies the following:
 - (a) The *firing condition* given by a predicate $c(m_1(t), \dots, m_p(t))$. If this is true, T gets ready to fire.
 - (b) The *delay function* given by a nonnegative integer valued function $d(m_1(t), \dots, m_p(t))$. If the firing condition gets satisfied at time t , T fires in delay $d(m_1(t), \dots, m_p(t))$. However, if the firing condition is changed during this delay time, the transition T loses the chance of firing and the firing condition will be reset.
 - (c) For each input arc a_i , T specifies a nonnegative integer valued function $f_i(m_1(t), \dots, m_p(t)) \geq 0$ which defines the the number of tokens (integer) removed from P_i through arc a_i by firing. If a_i is a test input arc, then we assume $f_i \equiv 0$ and no token is removed.
 - (d) For each output arc b_j , T specifies a nonnegative integer valued function $g_j(m_1(t), \dots, m_p(t)) \geq 0$ which defines the number of tokens (integer) are added to Q_j through arc b_j by firing.

In Figure 7, examples of continuous transition and discrete transition are shown.

From the above definition, it may be obvious that in the HFPN model, the dimer-to-monomers reaction can be intuitively represented as Figure 6 (c). Not only this simple example but also more complex interactions can be easily and intuitively described with HFPN. The software *Genomic Object Net* is developed and implemented based on this HFPN architecture.

2.2 Hierarchical Representation

Needless to say, hierarchization is a key concept for representing complex network structures. The hierarchical representation has been also introduced in the HDN model

by employing the object-oriented approach and this model is called the hybrid object net (HON) [3, 4]. We have used this hierarchical approach for representing the switching mechanism of λ phage with the HON model and realized a simple representation of the network with a prospective view [27]. In *Genomic Object Net*, the system for hierarchical representation is also implemented for the HFPN. An example may be enough for defining how hierarchical representation is realized in *Genomic Object Net*. Figure 8 (a) shows a screen snapshot of *Genomic Object Net* which describes the gene regulatory network of λ phage, where the part corresponding to the switching mechanism is hierarchically represented as explained in Figure 8 (b).

Design Principle of Biopathways with HFPN

Usually, in the literature, biopathway information is conceptually described as a schematic figure together with the explanation about the relations between biological objects of concern and the measured/observed data proving their qualitative/quantitative relations (e.g. Figure 9 (a), Figure 11 (a), Figure 14, Figure 19). It also implicitly provides us the scale and degrees of freedom in simulation.

Our principle for designing HFPN in biopathway modeling consists of the following items with which the information shall be easily described and modeled.

1. Identify “main events” in the biopathway of concern.
2. Identify “objects” related to the main events that should be represented as places (discrete or continuous) in a top-down manner. “Hidden objects” that are not explicitly mentioned should also be identified in this process (e.g. Figure 9 (b), Figure 11 (b)).
3. Identify “interactions between objects” and represent them as transitions (discrete or continuous). Also identify “hidden interaction”. Based on the logical structure in events and biological/biochemical knowledge about objects, the functions assigned to transitions shall be designed (e.g. Figure 9 (b), Figure 11 (b)-(c), Figure 12, Figure 16, Figure 20, Table 1).
4. Simulate the designed HFPN and evaluate the simulation result with a graphical visualization tool (e.g. Figure 13, Figure 17, Figure 18, Figure 21, Figure 23). Then tune up the parameters of the functions for transitions so that the simulation result shall be consistent with the biological fact/observation.
5. If necessary, hierarchical representation [27] shall be considered for more compact description (e.g. Figure 8 (a)-(b)).

Although this principle is rather rough, we shall show in Section 3 that we can describe some typical biopathways related to gene regulation (circadian rhythms of *Drosophila* and *lac* operon), metabolic pathway (glycolytic pathway of *E. coli*) and signal transductions (apoptosis induced by Fas ligand), which mostly cover the basic aspects in biopathways.

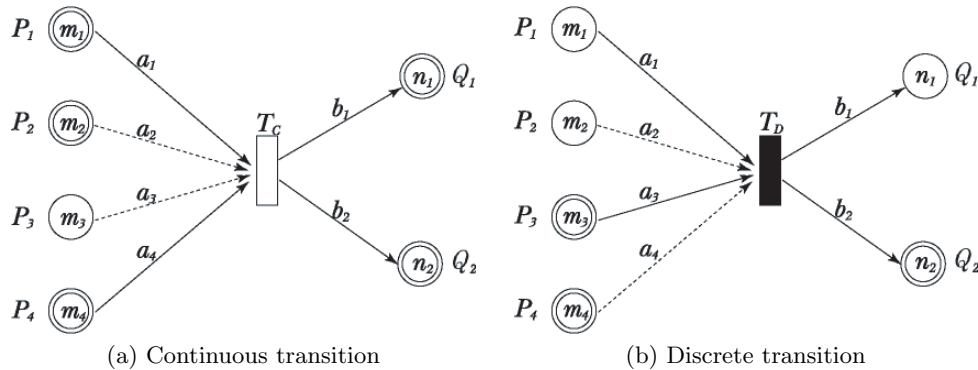


Fig. 7. Continuous and discrete Transitions of hybrid functional Petri net.

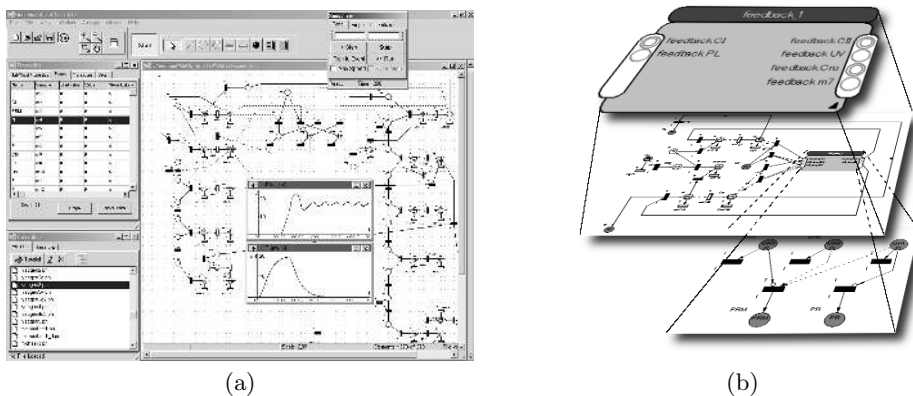


Fig. 8. (a) The gene regulatory network of λ phage described and simulated with *Genomic Object Net*. (b) Hierarchical construction of the λ phage genetic switch mechanism.

3 Modeling Biopathways with Genomic Object Net

In this section, we show representations and simulations of three biopathways: *lac* operon gene regulatory mechanism with the glycolytic metabolic pathway, circadian rhythm gene regulatory network of *Drosophila*, and Fas ligand induced apoptosis signaling network. All HFPN files of them can be downloaded from the URL [http : //www.GenomicObject.Net/](http://www.GenomicObject.Net/).

3.1 Metabolic Pathway: Glycolytic Pathway and *lac* Operon

As an example of metabolic pathway, we model the glycolytic pathway with HFPN that was first modeled with the discrete Petri net by Reddy [32]. Figure 10 and Table 1 show the pathway and the enzymes related to the reactions to model. Together with modeling of the glycolytic pathway, we will model the *lac* operon gene regulatory mechanism of *E. coli* with HFPN.

Figure 11 (a) shows the dual control of the *lac* operon participating *lac* repressor, allolactose, catabolite gene activator protein (CAP), and cyclic AMP (cAMP). *LacZ*, the first gene of the *lac* operon, encodes the enzyme β -galactosidase which breaks down lactose to galactose and glucose. The initiation of transcription of *lac* operon is controlled by the following mechanisms participating *lac* repressor protein and CAP: (1) lactose addition increases the concentration of allolactose which binds to the repressor protein and removes it from the DNA, and (2) glucose addition decreases the concentration of cAMP; because cAMP no longer binds to CAP, this gene activator dissociates from the DNA, turning off the operon.

The modeling is simply done by mapping the information represented in Figure 10 and Figure 11 (a) to places and transitions. The necessary parameters and functions for transitions were hand-tuned. There was, however, practically no difficulty in obtaining the HFPN representation in Figure 12 and its simulation of the concentration behaviors of glucose, lactose, *lacZ* protein, ATP, and pyruvic acid (Figure 13) shows that this model works reasonably. The modeling was done in two

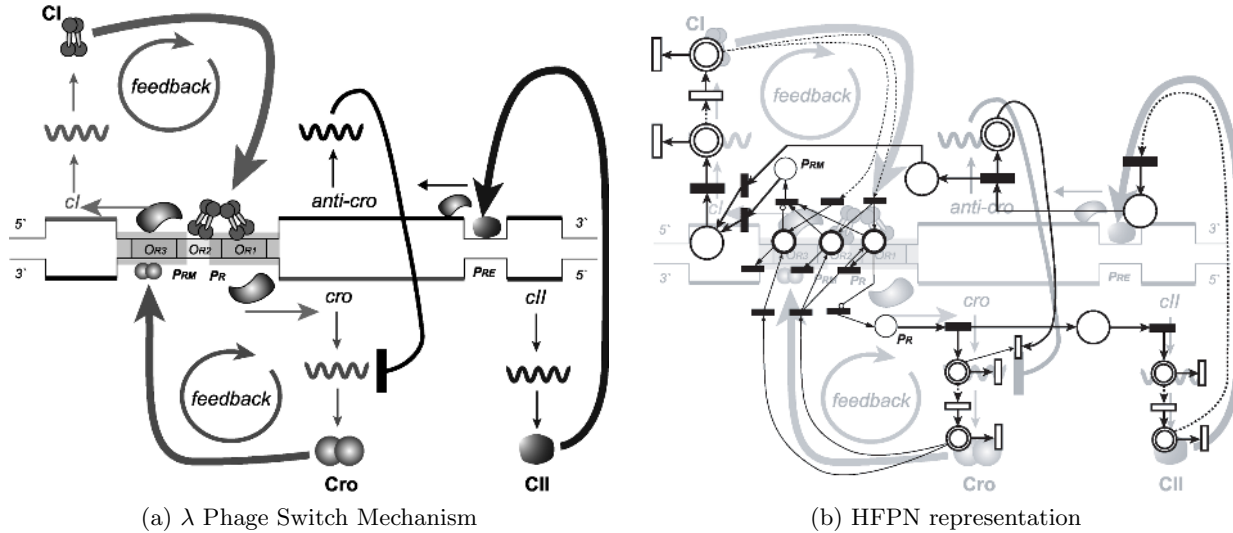


Fig. 9. A schematic description of the λ phage genetic switch feedback mechanism and its hybrid functional net representation: The genes *cro*, *cII* and the genes followed by *cII* will be transcribed from the promoter P_R , when neither CI protein nor Cro protein does not bind to the operator sites O_{R3} , O_{R2} , and O_{R1} . The condition of *E. coli* gives an effect to the concentration of CII protein. If the concentration of CII protein is low, the transcription from P_R continues and keeps the concentration of Cro protein at some level by the feedback control of the Cro protein itself. On the other hand, if the concentration of CII protein is high, the CII protein binds to the promoter P_{RE} as a positive transcription factor, then the transcription from P_{RE} begins. Then, anti-sense RNA of the gene *cro* is produced, which helps to degrade the concentration of Cro protein more rapidly. Transcription of *cI* gene is followed and concentration of CI protein keeps at some level by the feedback control of the CI protein itself.

parts. It should be noted that the modeling has benefited from the hybrid nature of continuous and discrete places/transitions and the new ability introduced to transition of HFPN in addition to the traditional features of Petri net.

Metabolic pathway: For each object in Figure 10 (ATP, ADP, enzyme for each reaction, Gluc, G6P, ..., Lac), a continuous place is created. The content of the place represents the concentration of the object. For each reaction in Figure 10, we define a continuous transition whose firing speed is given by the Michaelis-Menten's equation, where the parameters are roughly provided by setting $V_{max} = 1$ and $K_m = 1$. The natural degradation of compound is realized by a continuous transition without any outgoing arc which only consumes but does not produce any. The effect of an enzyme is represented with a test arc since it does not consume by the reaction. In the reaction 12 from FBP to GAP catalyzed by aldolase, a six-carbon sugar is cleaved to give two three-carbon sugars, and therefore the number of molecules is doubled. This reaction is described with the newly introduced function of HFPN, where continuous places *m28* and *m27* in Figure 12 represent the concentrations of FBP and GAP, respectively.

Gene regulation of the *lac* operon: A schematic explanation of the regulation mechanism (Figure 11 (a)) is directly translated to places and transitions (Figure 11 (b)). The places represent objects such as CAP, cAMP, cAMP/CAP-complex, *lac* repressor, lactose, galactose, allolactose, β -galactosidase, glucose, mRNAs, etc. whose contents represent the concentrations of the objects. The

functions defined for the transitions are again simply given by manual tuning according to logical structure and biochemical knowledge. The switching mechanism is realized by using discrete places, discrete transitions and test and inhibitory arcs in Figure 11 (c) in the following way: If the concentrations of CAP and cAMP exceed the levels w_c and w_A , respectively, the complex of CAP and cAMP is produced and binds to the CAP-binding site. In HFPN modeling, we set the test arc weights by $w_c = 1$ and $w_A = 1$ and discrete transition CAP/cAMP produces one token at each time while the contents of continuous places CAP and cAMP are not consumed because the arcs are test arcs except for the transitions representing degradation. Discrete place P_{comp} represents the CAP-binding site and its capacity (the number of maximum tokens held by the place) is set to be two. Discrete transition D_{comp} removes CAP/cAMP-complex from P_{comp} by one token at each time. In the same way, if the concentration of *lac* repressor exceeds the level w_ℓ while the concentration of allolactose does not exceed the level w_a , *lac* repressor binds to the operator site (represented by discrete place P_{rep}) which is removed from the site at the rate assigned to transition D_{rep} . Under the condition that the complex of CAP and cAMP binds at promoter site, i.e. P_{comp} holds at least one token, and *lac* repressor does not bind to the operator site, i.e. P_{rep} does not hold any token, the switch of *lac* operon transcription (represented by discrete place P_{ec}) will be turned on.

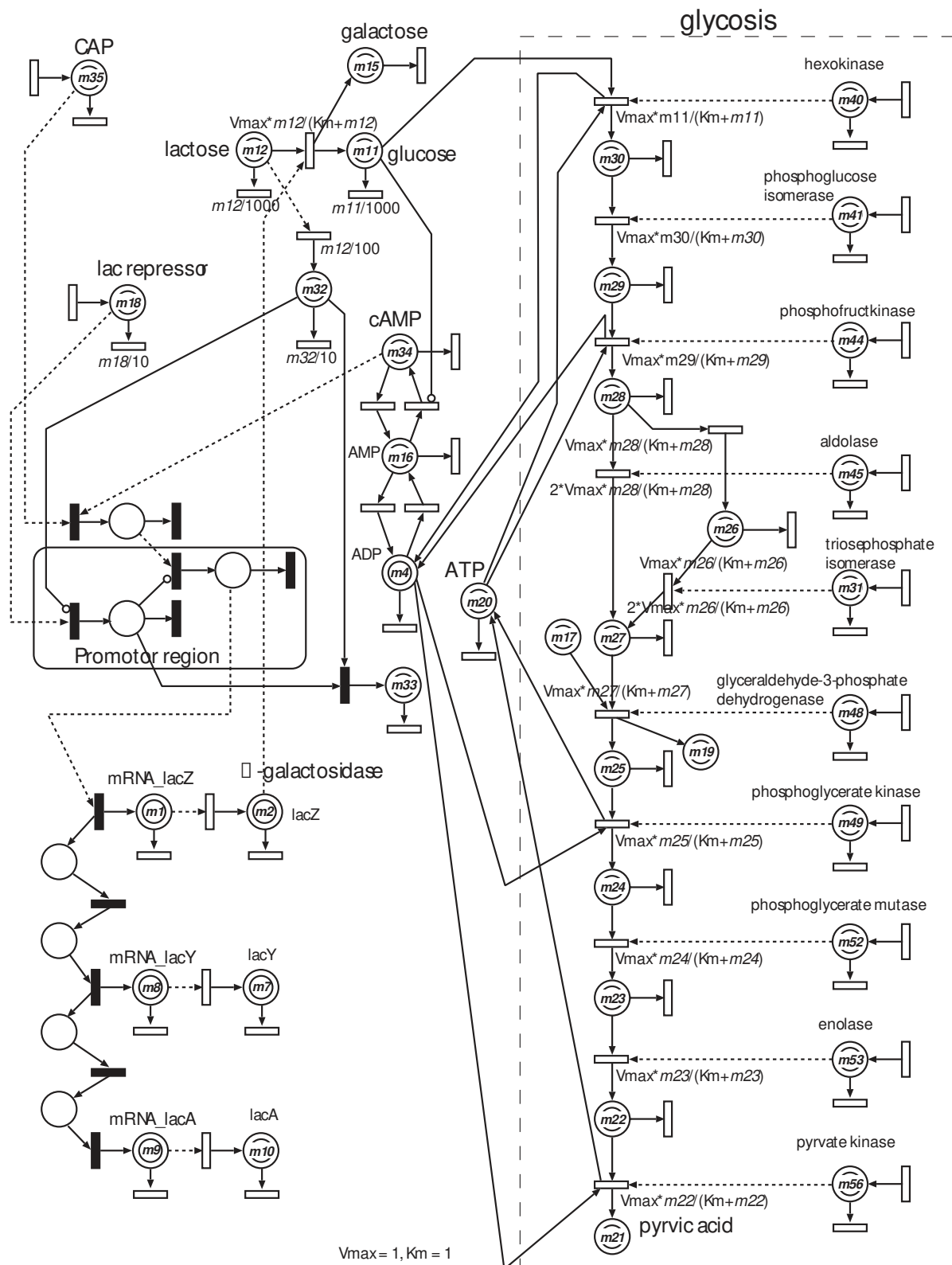
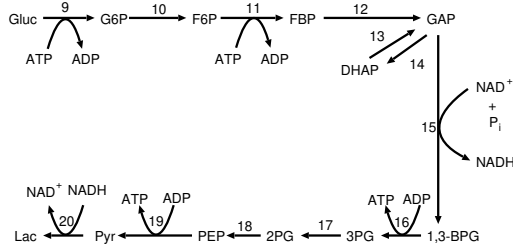


Fig. 12. A HFPN modeling of the glycolytic pathway and *lac* operon gene regulatory mechanism of *E. coli*. A HFPN file including all transition parameters can be downloaded from the URL <http://www.GenomicObject.Net>.

Table 1. Enzyme reactions: Index numbers correspond to the reaction numbers in Figure 10.

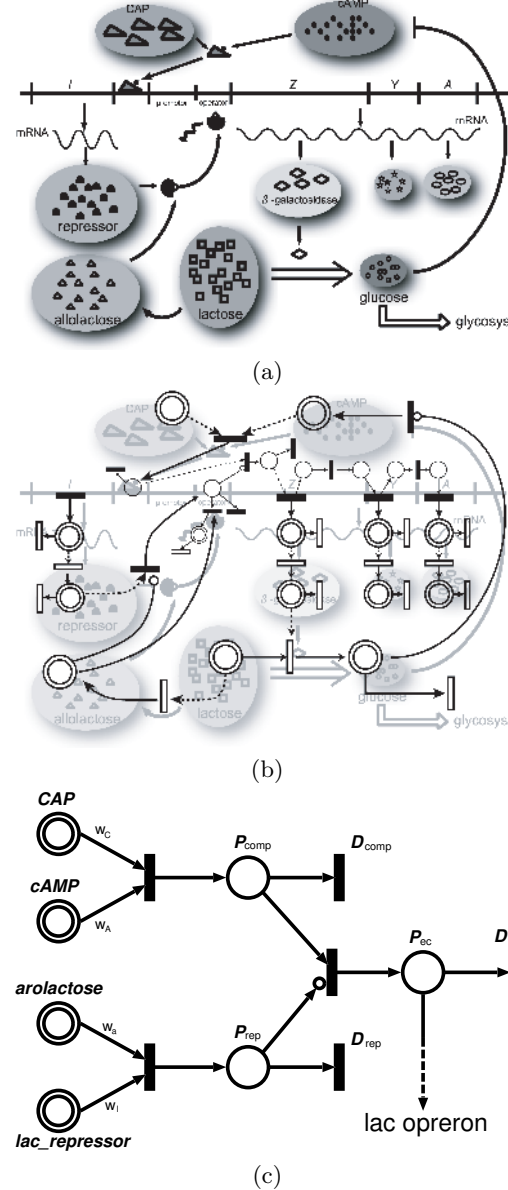
Index	Enzyme / Reaction	Index	Enzyme / Reaction
9	<i>hexokinase</i>	10	<i>phosphoglucose isomerase</i>
11	<i>phosphofructokinase</i>	12	<i>aldolase</i>
13	<i>triosephosphate isomerase</i>	14	<i>triosephosphate isomerase</i>
	(forward reaction)		(backward reaction)
15	<i>glyceraldehyde-3-phosphate dehydrogenase</i>	16	<i>phosphoglycerate kinase</i>
17	<i>phosphoglycerate mutase</i>	18	<i>enolase</i>
19	<i>pyruvate kinase</i>	20	<i>lactate dehydrogenase</i>

**Fig. 10.** A part of the glycolytic pathway.

3.2 Gene Regulation: Circadian Rhythms in *Drosophila*

The control mechanism of autoregulatory feedback loops of *Drosophila* circadian rhythms has been intensively studied [5, 7, 10, 21, 31, 43] and some fine modelings by ODEs with detailed coefficients have also been reported [24, 41]. These ODE-based models can be easily described with HFPNs with *Genomic Object Net*. Highly appreciating such fine modelings, we first show a HFPN realization of the model due to Ueda et al. [41]. Moreover, we also show that a HFPN can be designed with *Genomic Object Net* easily and intuitively by interpreting the biological facts and observations given in [5, 7, 10, 21, 31, 43]. *Genomic Object Net* is intended to be a naïve platform where we can create hypotheses and evaluate them by simulation. This feature is especially important when only rough modeling is enough or enough information is not available for fine modeling.

Figure 14 shows the scheme of the regulatory mechanism of five genes contributing to the *Drosophila* circadian rhythms; *period* (*per*), *timeless* (*tim*), *Drosophila Clock* (*dClk*), *cycle* (*cyc*) and *double-time* (*dbt*). It is known that the *Drosophila* circadian feedback system is composed of two interlocked negative feedback loops [7]. Roughly speaking, PER and TIM proteins collaborate in the regulation of their own expression in *Drosophila*, assembling in PER-TIM complexes that permit nuclear translocation, inactivation of *per* and *tim* transcription in a cycling negative feedback loop, and activation of *dClk* transcription which participates in the dCLK-CYC negative feedback loop. The dCLK and CYC form heterodimers that activate *per* and *tim* transcriptions and

**Fig. 11.** (a) The dual control of the *lac* operon. (b) A HFPN realization of the regulatory mechanism. (c) The switching mechanism realized with discrete places, transitions and test arcs.

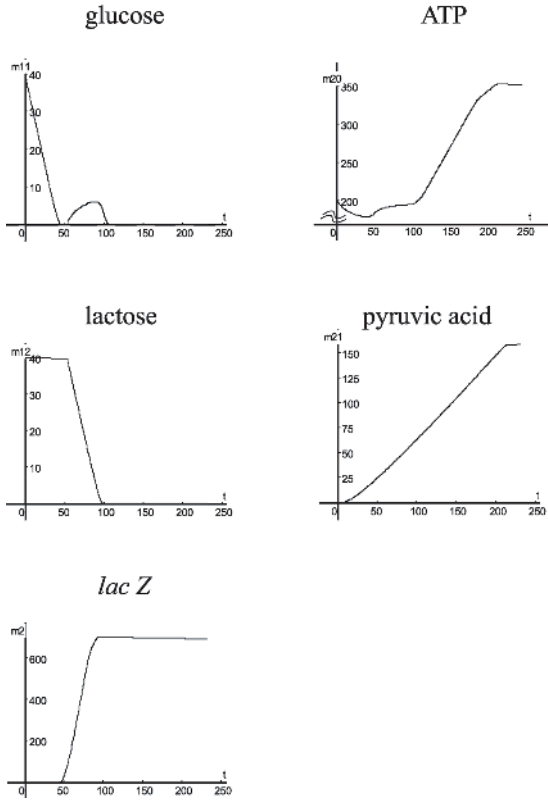


Fig. 13. This figure shows the behaviors of concentrations of glucose, lactose, *lacZ*, ATP, and pyruvic acid. As soon as the glucose is almost consumed (around time 20), the production of *lacZ* protein is begun. When the concentration of *lacZ* protein reaches at some level (around time 35), the concentration of glucose begins to increase again resulting from breaking down the lactose to the glucose and galactose. At the time when the lactose almost disappears (around time 55), the transcription of *lacZ* gene is stopped. Growths of the concentrations of ATP and pyruvic acid are also observed in the figure.

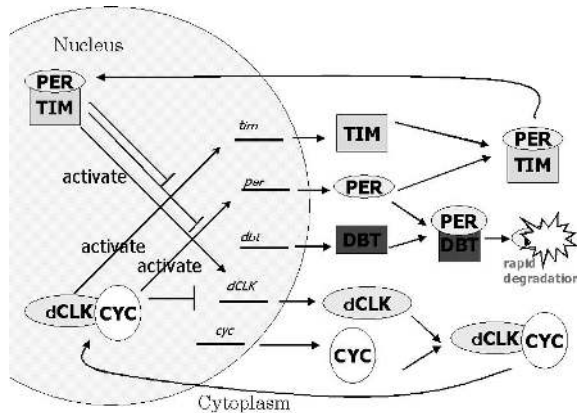


Fig. 14. The gene regulation in the *Drosophila* circadian oscillator is schematized.

inhibit *dClk* transcription. Among these five genes, three genes, *per*, *tim*, and *dClk*, are rhythmically expressed: *per* and *tim* mRNA levels begin to rise in the subjective day and to peak early in the subjective evening, and *dClk* mRNA level peaks late at night to early in the morning. Although *per* and *tim* mRNAs reach peak levels in the evening, PER and TIM levels do not peak until late evening. It is considered that this delay results from the initial destabilization of PER by DBT-dependent phosphorylation followed by the stabilization of PER by dimerization with TIM [21,31]. The details of the mechanism are surveyed in [5,10,43].

Ueda et al. [41] have modeled the two interlocked negative feedback loop system [7] with ODEs and made extensive simulation and mathematical analysis. We have translated it into a HFPN as in Figure 15 and further computational experiments based on this model are possible on *Genomic Object Net* with this HFPN file.

By using *Genomic Object Net*, we also designed a HFPN from scratch by interpreting the facts and observations in [5,7,10,21,31,43]. Figure 16 is a naïve representation of the gene regulatory mechanism of *Drosophila* circadian oscillator, where continuous places are introduced in the same way as Section 3.1 and the functions for continuous transitions are defined and tuned so that the simulation results will coincide with the facts and observations. In Figure 16, smaller value of tokens *m2* or *m4* is taken as the complex forming rate of the proteins dCLK (*m2*) and CYC (*m4*) at the transition *T1*. *Genomic Object Net* can assign a perl script to any transition for realizing such a sophisticated function. The perl script of this case describes the program which takes smaller ones of tokens *m2* or *m4*. Complex forming rates of PER/TIM and PER/DBT are similarly realized at the transitions *T2* and *T3*, respectively, by using this function. Transitions *T4*, *T5*, and *T6* represent the degradation rates of complexes of the corresponding proteins. Figure 17 (a) is the simulation result of the HFPN in Figure 16. It indicates that this HFPN model representing two negative feedback loops, the PER-TIM feedback and the dCLK-CYC feedback, successfully produce periodic oscillations of *per* mRNA (*m6*), *tim* mRNA (*m8*), and *dClk* mRNA (*m1*), while the concentration of *cyc* mRNA (*m3*) keeps constant expression.

It is known that the protein TIM stabilizes phosphorylated PER by dimerizing with it. This phenomenon is reflected to the firing speed of transition *T5*, that is, the firing speed of transition *T5* (*m13/15*) is set to be slower than the one of transition *T7* (*m7/10*). Moreover, it is suggested in [31] that the normal function of protein DBT is to reduce the stability and thus the level of accumulation of monomeric PER proteins. This function is realized in Figure 16 in transition *T3*. It is clearly expressed in Figure 17 (b) that there is time difference around four hours between the peaks of concentrations of *per* mRNA and PER which is believed to be arisen from the above two facts. This indicates that the result

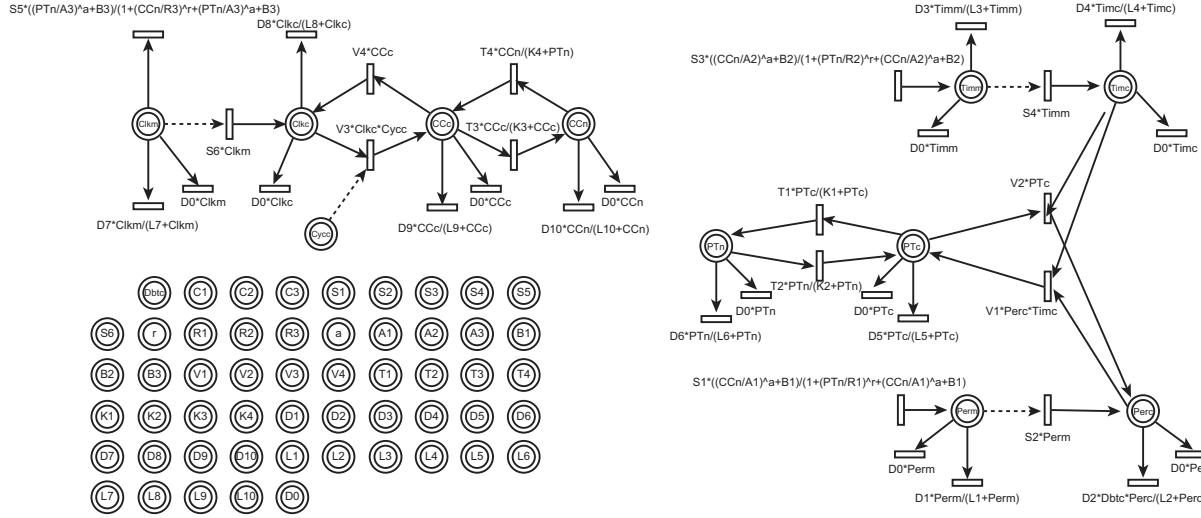


Fig. 15. A HFPN realization of the circadian rhythm model due to Ueda et al. [41]. A series of ten ODEs, e.g. $\frac{dPer_m}{dt} = C_1 + S_1 \frac{\left(\frac{CC_n}{A_1}\right)^a + B_1}{1 + \left(\frac{PT_n}{R_1}\right)^r + \left(\frac{CC_n}{A_1}\right)^a + B_1} - D_1 \frac{Per_m}{L_1 + Per_m} - D_0 Per_m$, are realized in this network, where Per_m (CC_n , PT_n) represents the concentration of *per* mRNA (dCLK-CYC complex in the nucleus, PER-TIM complex in the nucleus) and $C_1 = 0\text{nM/h}$, $S_1 = 1.4\text{nM/h}$, $A_1 = 0.45\text{nM/h}$, $B_1 = 0$, $L_1 = 0.3\text{nM/h}$, $D_0 = 0.012\text{nM/h}$, $D_1 = 0.94\text{nM/h}$, $R_1 = 1.02\text{nM/h}$.

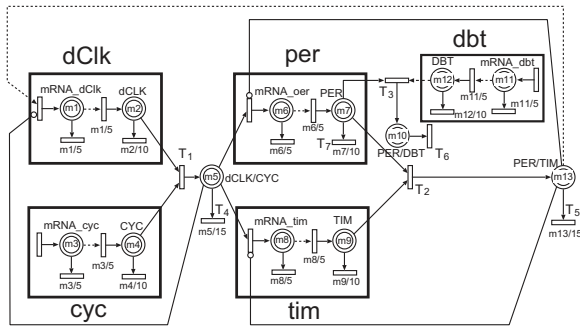


Fig. 16. A naïve HFPN representation of *Drosophila* circadian mechanism in which five genes *per*, *tim*, *dClk*, *cyc*, and *dbt* participate. A HFPN file including all transition parameters can be downloaded from the URL <http://www.GenomicObject.Net>.

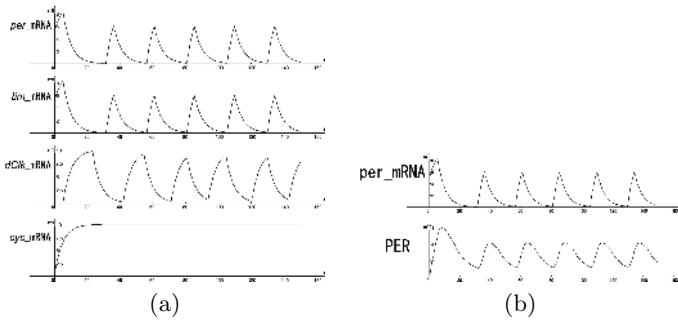


Fig. 17. (a) Behaviors of concentrations of four mRNAs simulated on *Genomic Object Net*. (b) Time difference around four hours is observed between the peaks of concentrations of *per* mRNA and PER.

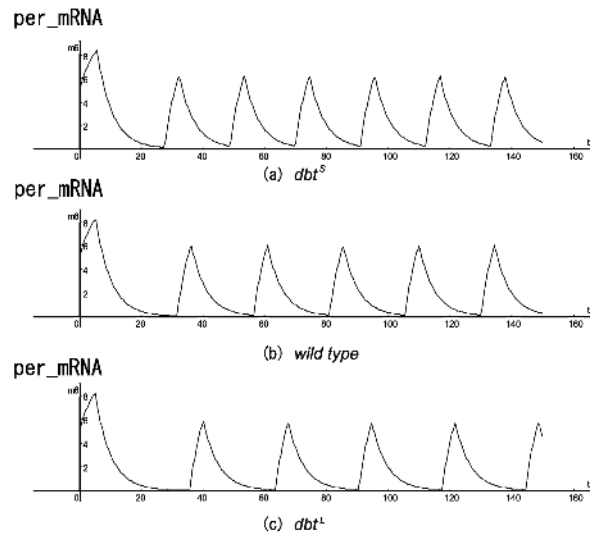


Fig. 18. Concentration behaviors of *per* mRNA. (a) dbt^L mutant (b) Wild type (c) dbt^S mutant

of simulation is in good agreement with the experimental observation reviewed in [10].

3.3 Signal Transduction: Apoptosis Induced by Fas ligand

The purpose of this section is to show that *Genomic Object Net* based on HFPN is useful to model signal transduction pathways. We considered the biopathways known for the apoptosis induced by Fas ligand and made a computational experiment for evaluating the effect of autocatalytic process.

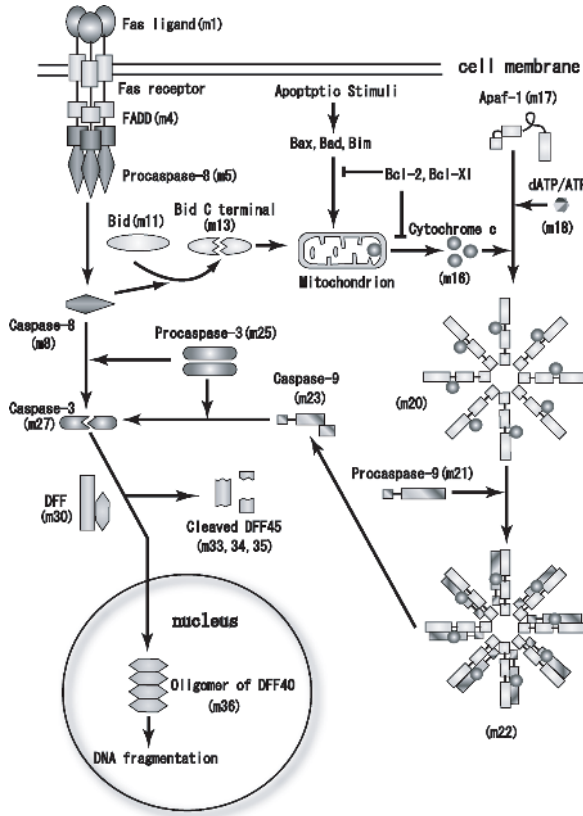


Fig. 19. Proposed steps of apoptosis induced by Fas ligand.

Apoptosis, programmed cell death, is known to participate in various biological processes such as development, maintenance of tissue homeostasis and elimination of cancer cells [18,38]. Malfunctions of apoptosis have been implicated in many forms of human diseases such as neurodegenerative diseases, AIDS and ischemic stroke. Reportedly, apoptosis is caused by various inducers such as chemical compounds, proteins or removal of nerve growth factor. The biochemical pathways of apoptosis are complex and depend on both the cells and the inducers.

Fas-induced apoptosis has been studied in detail and its mechanism has been proposed as shown in Figure 19 [30]. Fas ligands, which usually exist as trimers, bind and activate their receptors by inducing receptor trimerization. Activated receptors recruit adaptor molecules such as Fas-associated protein with death domain (FADD), which recruit procaspase 8 to the receptor complex, where it undergoes autocatalytic activation. Activated caspase 8 activates caspase 3 through two pathways; The complex one is that caspase 8 cleaves Bcl-2 interacting protein (Bid) and its COOH-terminal part translocates to mitochondria where it triggers cytochrome c release. The released cytochrome c bind to apoptotic protease activating factor-1 (Apaf-1) together with dATP and procaspase 9 and activates caspase 9. The caspase 9 cleaves procaspase 3 and activates caspase 3. The other path-

way is that caspase 8 cleaves procaspase3 directly and activates it. The caspase 3 cleaves DNA fragmentation factor (DFF) 45 in a heterodimeric factor of DFF40 and DFF45. Cleaved DFF45 dissociates from DFF40, inducing oligomerization of DFF40 that has DNase activity. The active DFF40 oligomer causes the internucleosomal DNA fragmentation, which is an apoptotic hallmark indicative of chromatin condensation.

We described this mechanism as a HFPN with *Genomic Object Net*. The pathways consist of several steps where two different pathways from caspase 8 are assumed and many molecules including Fas receptors, caspase family which includes aspartic acid-dependent cysteine proteases and produced from their zymogens, Bcl-2 family which includes pro- and anti-apoptotic proteins, cytochrome c and DNA fragmentation factor. The apoptosis starts from the Fas ligand binding to Fas receptors and ends in the fragmentation of genomic DNA, which is used as a hallmark of apoptosis. Thus the amount of DNA fragmentation can be assumed to be proportional to the cell death.

In the same way as in Section 3.1 and Section 3.2, we have designed a HFPN by using the facts about the Fas-induced apoptosis pathways shown in Figure 19 and biochemical knowledge about reactions. Figure 20 shows the whole HFPN representation that we have described with *Genomic Object Net*. All places/transitions are continuous and parameters are roughly tuned by hands. For Bid (m11), Procaspase-9 (m21), Procaspase-3 (m25), DFF (m30), DNA (m37), the initial concentration of each compound is assumed to be 100. On the other hand, for FADD (m4), Procaspase-8 (m5), Apaf-1 (m17), dATP/ADP (m18), when two compounds react together without the stimulation of apoptosis, the initial concentrations and the rate are assumed to be 39.039 and $m1 * m2 / 5000$, respectively to keep the stable state condition. Each compound is assumed to be produced by the rate of 0.5 (represented by a transition without any incoming arc) and to degrade by the rate of its concentration divided by 200 (represented by a transition without any outgoing arc), which will keep its concentration at 100 under the stable state condition. This degradation rate also applies to other compounds in the network. The rate of other processes are determined roughly by following Table 2. Synthesis and catabolism processes are added in the model for all proteins. Autocatalytic processes are also added in the model to all caspases since they exist as proenzymes. The pathway from caspase 8 to caspase 3 is assumed when the caspase 8 concentration is over 30. Protease is often synthesized as a proenzyme (zymogen) and changed to active form by other enzymes or by itself. So autocatalytic process is added to every caspase reaction.

By using the apoptosis scheme modeled as a HFPN, we simulated the DNA fragmentation amount by varying the Fas ligand concentration and Figure 21 shows the simulated relationship. It shows that under very weak

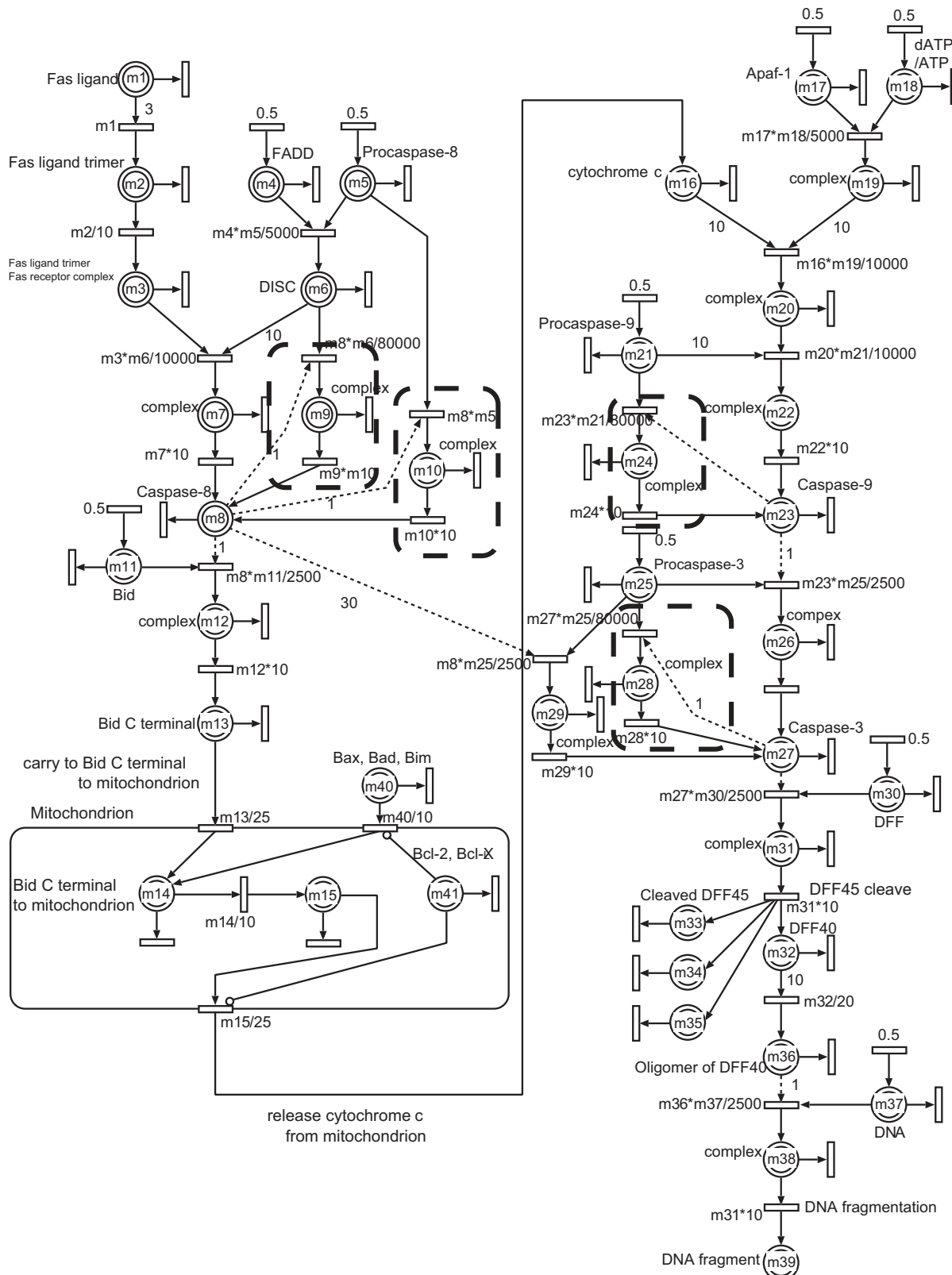


Fig. 20. A HFPN representing the Fas-induced apoptosis by HFPN obtained from Figure 19. Autocatalytic processes (Figure 22) are surrounded by bold dotted lines. A HFPN file including all transition parameters can be downloaded from the URL [http : //www.GenomicObject.Net](http://www.GenomicObject.Net).

Table 2. Functions assigned to continuous transitions in the simulation of apoptosis induced by Fas ligand, where mA and mB represent the contents of the corresponding continuous places.

Rate	Unimolecular reaction	Bimolecular reaction
Self-effacement	$mA/200$	
Oligomer	$mA/20$	$mA * mB/10000$
Monomer	$mA/10$	$mA * mB/5000$
Enzyme binding	$mA/5$	$mA * mB/2500$
Enzyme reaction	$mA * 10$	

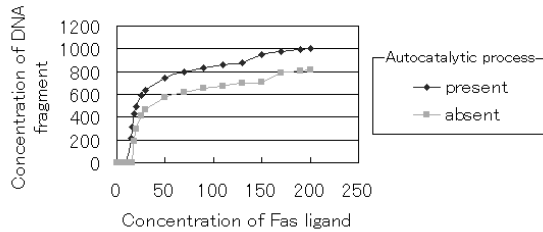


Fig. 21. Simulated relationship between the DNA fragmentation amount and the Fas ligand concentration: At higher concentration of Fas ligand, the direct pathway from caspase 8 to caspase 3 contributes to the fragmentation. To examine the effect of autocatalytic process of caspases, DNA fragmentation is simulated for both cases of the presence and absence in this process.

stimulation (very low amount of Fas ligand), DNA fragmentation does not occur since the stimulation stops at the intermediate point because of the assumption of degradation processes. With the increase of the stimulation, the reaction proceeds to the backward intermediates and DNA fragmentation (cell death) occurs finally, which increases with the increase of the Fas ligand concentration.

There are two pathways from activated caspase 8 to caspase 3, one through several steps including the cytochrome c release from mitochondria when the concentration of activated caspase 8 is low, and the direct one to caspase 3 when the concentration of activated caspase 8 is high [22]. We assume arbitrarily that the direct pathway starts when the concentration of activated caspase 8 is larger than 30. Reportedly the removal of the Bid by gene knockout method increases the resistance of liver cell apoptosis by Fas ligand, while it does not affect the apoptosis of thymus and embryonic cells. If the second pathway is included to the scheme, DNA fragmentation increases slightly, especially, when the Fas ligand concentration is high (Figure 21). However the detailed mechanism of the selection of these two pathways from caspase 8 are still unclear and necessary to be studied in future in the laboratory.

Since the presence of autocatalytic process is proposed in caspases [17], it is included in our model (Figure 22), which increases the DNA fragmentation as shown in Figure 21. However, if the large rate of the autocatalytic process is assumed in the caspase reaction, the

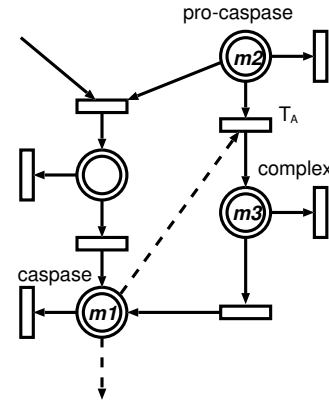


Fig. 22. A HFPN representation of autocatalytic process in Figure 20.

Table 3. DNA fragmentation at four autocatalytic rates of caspases ($rate0=0$, $rate1=mA*mB/8000$, $rate2=mA*mB/4000$, and $rate3=mA*mB/2500$), which are assigned to the transition T_A in Figure 22. The stop time represents the period after that Fas ligand stimulation is stopped. The initial Fas ligand concentration is set to be $n = 200$. Variables mA and mB represent the contents of the continuous places going into T_A .

DNA Fragmentation				
Stop time	rate0	rate1	rate2	rate3
10	0	0	0	779
15	0	405	715	1824
20	402	567	869	2025

DNA fragmentation becomes independent of the Fas ligand concentration, which disagrees with the experimental results. Therefore, we can guess that autocatalytic processes must be slow if they are at present. To examine the effect of autocatalytic processes of caspases on the apoptosis by Fas ligand, DNA fragmentation is simulated when the stimulation by Fas ligand stopped after a short period. Table 3 shows a simulation result that the apoptosis proceeds more with the increase of the autocatalytic rate of caspases even for a short period stimulation.

Figure 23 shows simulated time courses of the HFPN in Figure 20 with *Genomic Object Net*. Some intermediates during apoptosis at three levels of Fas ligand concentrations are measured. These time courses might be useful to plan new experiments such as addition of inhibitors to some step. However, it is necessary to estimate the realistic rates of each reaction by the comparison with the experimental data. It is also necessary to add other pathways through Bcl-2 family or p53 to describe the real apoptosis held in various cells and by various inducers.

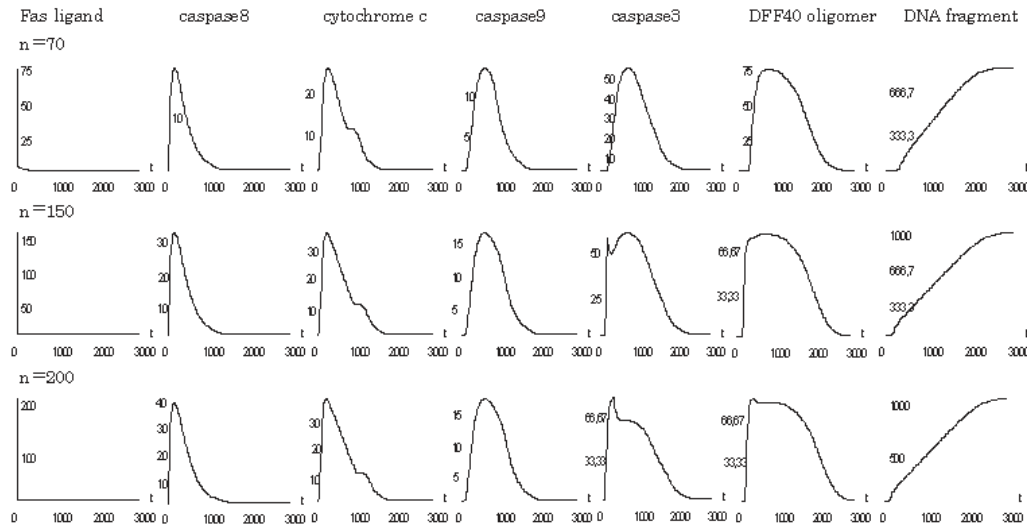


Fig. 23. Simulated time courses of some intermediates during apoptosis for the Fas ligand concentration $n = 70, 150, 200$.

4 Concluding Remarks

Not only for ODEs but also for HFPNs, optimizing parameters is the important issue for obtaining appropriate biopathways models. In the HFPN biopathways modeled in this paper, we hand-tuned all parameters to the aimed biological behaviors. Note that, in Genomic Object Net, hand-tuning processes are rather smooth than the same processes in other biosimulation tools such as E-Cell and BioDrive, since Genomic Object Net has an excellent user-interface which allows us to directly change parameters described in HFPN biopathway models. However, for making Genomic Object Net more powerful, parameter tuning mechanism is going to be integrated in the next version.

In E-CELL, a system of biopathways is represented with a spread sheet compiling substances and reactions with ordinary differential equations (ODEs). For reactions which cannot be represented with ODEs, it employs *ad hoc* user-defined C++ programs called postern reactor. In the following, we show a rough sketch of procedure for obtaining HFPN by converting E-CELL biopathway models.

1. Assign a continuous place to each of substances in E-CELL spread sheet,
2. describe HFPNs which correspond with all E-CELL reactors,
3. combine HPFNs obtained above at a continuous place of common substance in two (or more) E-CELL reactors, and
4. determine firing speeds of continuous transitions by referring constants described in E-CELL spread sheet.

A conversion program from E-CELL to *Genomic Object Net* is now being developed.

References

1. Alla, H. and David, R. (1998) Continuous and hybrid Petri nets. *Journal of Circuits, Systems, and Computers*, **8**(1), 159–188.
2. Arkin, A., Ross, J., and McAdams, H.H. (1998) Stochastic kinetic analysis of developmental pathway bifurcation in phage lambda-infected *Escherichia coli* cells. *Genetics*, **149**, 1633–1648.
3. Drath, R. (1998) Hybrid object nets: An object oriented concept for modeling complex hybrid systems. *Proc. Hybrid Dynamical Systems, 3rd International Conference on Automation of Mixed Processes, ADPM'98*, 437–442. [http : //www.systemtechnik.tu – ilmenau.de/ drath/Download/Reims98.zip](http://www.systemtechnik.tu-ilmenau.de/~drath/Download/Reims98.zip)
4. Drath, R., Engmann, U. and Schwuchow, S. (1999) Hybrid aspects of modeling manufacturing systems using modified Petri nets. In: *5th Workshop on Intelligent Manufacturing Systems*, Granado, Brasil. [http : //www.systemtechnik.tu – ilmenau.de/ drath/Download/Brasil98.ps.zip](http://www.systemtechnik.tu-ilmenau.de/~drath/Download/Brasil98.ps.zip)
5. Dunlap, J.C. (1999) Molecular bases for circadian clocks, *Cell* **96**, 271–290.
6. Genrich, H., Küffner, R. and Voss, K. (2001) Executable Petri net models for the analysis of metabolic pathways, *International Journal on Software Tools for Technology Transfer*, **3**(4), 394–404.
7. Glossop, N.R.J., Lyons, L.C., Hardin, P.E. (1999) Interlocked feedback loops within the *Drosophila* circadian oscillator, *Science* **286**, 766–768.
8. Goss, P.J.E. and Peccoud, J. (1998) Quantitative modeling of stochastic systems in molecular biology by using stochastic Petri nets. *Proc. Natl. Acad. Sci. USA*, **95**, 6750–6755.
9. Goss, P.J.E. and Peccoud, J. (1999) Analysis of the stabilizing effect of Rom on the genetic network controlling ColE1 plasmid replication. *Proc. Pacific Symposium on Biocomputing '99*, 65–76.

10. Hardin P.E. (2000) From biological clock to biological rhythms. *Genome Biology* 2000, **1**(4), reviews1023.1-1023.5.
11. Heiner, M., Koch, I. and Voss, K. (2001) Analysis and simulation of steady states in metabolic pathways with Petri nets. *Third Workshop and Tutorial on Practical Use of colored Petri Nets and CPN Tools*, Univ. of Aarhus, DAIMI PB-554, 15-34.
12. Heinrich, R. and Schuster, S. (1996) The regulation of cellular systems. Chapman & Hall, New York.
13. Heinrich, R. and Schuster, S. (1998) The modelling of metabolic systems. Structure, control, and optimality. *BioSystems* **47**, 61-77.
14. Heidtke, K.R. and Schulze-Kremer, S. (1998) Design and implementation of qualitative simulation model of λ phage infection. *Bioinformatics*, **14**, 81-91.
15. Hofestädt, R. (1994). A Petri net application of metabolic processes. *J. System Analysis, Modelling and Simulation* **16**, 113-122.
16. Hofestädt, R. and Thelen, S. (1998) Quantitative modeling of biochemical networks. *In Silico Biology*, **1**. [http : //www.bioinfo.de/isb/1998/01/0006/](http://www.bioinfo.de/isb/1998/01/0006/)
17. Hugunin, M., Quintal, L.J., Mankovich, J.A. and Ghayur, T. (1996) Protease activity of in vitro transcribed and translated *Caenorhabditis elegans* cell death gene (*ced-3*) product. *Journal of Biological Chemistry*, **271**, 3517-3522.
18. Jacobson, M.D., Weil, M. and Raff, M.C. (1997) Programmed cell death in animal development, *Cell* **88**, 347-354.
19. Kohn, M.C. and Lemieux, D.R. (1991) Identification of regulatory properties of metabolic networks by graph theoretical modeling. *Journal of Theoretical Biology*, **150**, 3-25.
20. Kanehisa, M. and Goto, S. (2000) KEGG: kyoto encyclopedia of genes and genomes. *Nucleic Acids Res.* **28**(1), 27-30.
21. Kloss, B., Price, J.L., Saez, L., Blau, J., Rothenfluh, A., Wesley, C.S. and Young, M.W. (1998) The *Drosophila* clock gene double-time encodes a protein closely related to human casein Kinase I ϵ . *Cell* **94**, 97-107.
22. Kuwana, T., Smith, J.J., Muzio, M., Dixit, V., Newmeyer, D.D., and Kornbluth, S. (1998) Apoptosis induction by caspase-8 is amplified through the mitochondrial release of cytochrome c. *Journal of Biological Chemistry*, **273**, 16589-16594.
23. Kyoda, K., Muraki, M. and Kitano, H. (2000) Construction of a generalized simulator for multi-cellular organisms and its application to Smad signal transduction, *Proc. Pacific Symposium on Biocomputing 2000*, 317-329.
24. Leloup, J-C. and Goldbeter, A. (1998) A model for circadian rhythms in *Drosophila* incorporating the formation of a complex between the PER and TIM proteins, *J. Biol. Rhythms*, **13** (1), 70-87.
25. Mangold, M., Kienle, A., Mohl, K.D., and Gilles, E.D. (2000) Nonlinear computation using DIVA - methods and applications, *Chem. Eng. Sci.* **55**, 441-454.
26. McAdams, H.H. and Arkin, A. (1997) Stochastic mechanisms in gene expression. *Proc. Natl. Acad. Sci. USA*, **94**, 814-819.
27. Matsuno, H., Doi A., Nagasaki M. and Miyano, S. (2000) Hybrid Petri net representation of gene regulatory network. *Proc. Pacific Symposium on Biocomputing 2000*, 338-349.
28. Mendes, P. (1993) GEPASI: a software for modeling the dynamics, steady states and control of biochemical and other systems, *Comput. Appl. Biosci.*, **9**(5), 563-571.
29. Meric, P.A. and Wise, M.J. (1998) Quantitative scalable discrete-event simulation of metabolic pathways. *Intelligent Systems for Molecular Biology*, AAAI Press, 187-194.
30. Nijhawan, D., Honarpour, N. and Wang, X. (2000) Apoptosis in neural development and disease. *Annual Reviews of Neuroscience*, **23**, 73-87.
31. Price, J.L., Blau, J., Rothenfluh A., Adobeely, M., Kloss, B. and Young, M.W. (1998) double-time is a novel *Drosophila* clock gene that regulates PERIOD protein accumulation, *Cell* **94**, 83-95.
32. Reddy, V.N., Mavrovouniotis, and Liebman, M.N. (1993), Petri net representations in metabolic pathways, *Proc. First ISMB*, 328-336.
33. Shaff, J. and Loew, L.M. (1999) The virtual cell. *Proc. Pacific Symposium on Biocomputing 1999*, 228-239.
34. Smaglik, P. (2000) For my next trick.... *Nature* **407**, 828-829.
35. Stelling, J., Kremling, A. and Gilles, E.D. (2000) Towards a virtual biological laboratory. *Proc. The First International Conference on Systems Biology*, 29-38 (to appear in "Foundations of Systems Biology", Kitano, H. (ed), MIT Press).
36. Stokes, C.L. (2000) Biological systems modeling: powerful discipline for biomedical e-R&D, *AIChe J.* **46**, 430-433.
37. Tomita, M., Hashimoto, K., Takahashi, K., Shimizu, T., Matsuzaki, Y., Miyoshi, F., Saito, K., Tanida, S., Yugi, K., Venter, J.C. and Hutchison, C. (1999) E-CELL: Software environment for whole cell simulation, *Bioinformatics*, **15**, 72-84.
38. Thompson, C.B. (1995) Apoptosis in the pathogenesis and treatment of disease, *Science* **267**, 1456-1462.
39. Tomita, M. (2001) Whole-cell simulation; a grand challenge of the 21st century, *Trends Biotechnol* **19**(6), 205-210.
40. Tomita, M. et al. (2000) The E-cell project: Toward integrative simulation of cellular processes, *Proc. 4th Annual International Conference on Computational Molecular Biology*, 290-298.
41. Ueda, H.R., Hagiwara, M., and Kitano, H. (2001) Robust oscillations within the interlocked feedback model of *Drosophila* circadian rhythm, *J. Theor. Biol.*, **210** (4), 401-406.
42. Valk, R. (1978) Self-modifying nets, a natural extension of Petri nets. *Lecture Notes in Computer Science*, **62** (ICALP '78), 464-476.
43. Young, M.W. (2000) Marking time for a kingdom, *Science* **288**, 451-453.
44. [http : //www.Biopathways.org/](http://www.Biopathways.org/)
45. [http : //genomics.lbl.gov/~aparkin/Group/Codebase/BioSpice/BioSpice.html](http://genomics.lbl.gov/~aparkin/Group/Codebase/BioSpice/BioSpice.html)